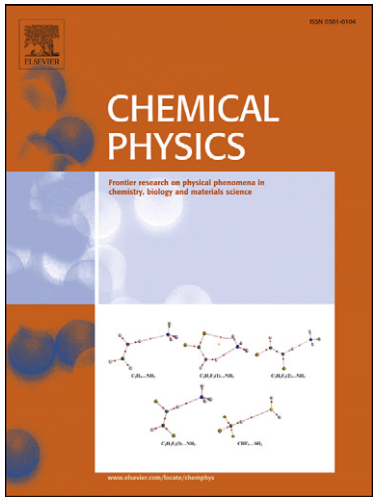

Contact geometry and electronic transport properties of Ag-benzene-Ag molecular junctions

Yang Li, Peng Wei, Meilin Bai, Ziyong Shen, Stefano Sanvito, Shimin Hou

PII: S0301-0104(12)00018-3
DOI: 10.1016/j.chemphys.2012.01.006
Reference: CHEMPH 8462

To appear in: *Chemical Physics*

Received Date: 19 November 2011
Accepted Date: 11 January 2012

Please cite this article as: Y. Li, P. Wei, M. Bai, Z. Shen, S. Sanvito, S. Hou, Contact geometry and electronic transport properties of Ag-benzene-Ag molecular junctions, *Chemical Physics* (2012), doi: 10.1016/j.chemphys.2012.01.006

Contact geometry and electronic transport properties of Ag-benzene-Ag molecular junctions

Yang Li[1], Peng Wei[1], Meilin Bai[1], Ziyong Shen[1], Stefano Sanvito[2], Shimin Hou[1*]

1 Centre for Nanoscale Science and Technology, Key Laboratory for the Physics and Chemistry of Nanodevices, Department of Electronics, Peking University, Beijing 100871, China

2 School of Physics and CRANN, Trinity College, Dublin 2, Ireland

Abstract

The contact geometry and the electronic transport properties of Ag-benzene-Ag molecular junctions have been investigated by using first-principles quantum transport simulations. Our calculations show that a moderate benzene-silver interaction can be achieved when benzene is adsorbed on the Ag(111) surface through adatoms. In this case three symmetric Ag-benzene-Ag junction models can be constructed, in which the molecule is connected to the electrodes through one or two Ag adatoms on each side. Although the contribution to the transmission around the Fermi level made by benzene molecular orbitals depends on the number of Ag adatoms and the detailed binding configuration, the transmission coefficients at the Fermi level of the three junctions are calculated to be respectively 0.20, 0.18 and 0.16. These values are well consistent with the experimental one of 0.24±0.08. Our results thus demonstrate that the conductance of Ag-benzene-Ag junctions is rather stable regardless of the molecule/electrode contact geometry.

Keywords: molecular junctions; contact geometry; benzene-silver interactions; non-equilibrium Green's function; density functional theory

* The corresponding author. E-mail: smhou@pku.edu.cn

1. Introduction

Molecular electronic devices, in which a single organic molecule is used as the active device component, have the potential of complementing and/or replacing the conventional silicon-based microelectronic devices [1,2]. Besides the quantum nature of the molecule and the band structures of the electrodes near the Fermi level (E_F), the electronic coupling at the molecule-electrode interface plays an important role in determining the transport properties of molecular devices. Although linker groups such as thiol, amine and isocyanide are always employed to wire the target molecule to the metal electrodes [3-8], recently much attention has been focused on connecting molecules to the electrodes directly [9-13]. For example, Kaneko et al. have successfully fabricated single benzene molecular junctions using Ag electrodes [10], where the evidence for the junction formation is provided by peaks in the inelastic electron tunneling spectroscopy (IETS) spectrum that cannot be attributed either to the Ag electrodes or to the benzene molecule. In contrast to the Pt-benzene-Pt junction which shows conductance values ranging from 1.0 G_0 to 0.1 G_0 [9], the Ag-benzene-Ag junction shows a stable conductance value of 0.24±0.08 G_0 [10] (here, $G_0 = \frac{2e^2}{h}$ is the conductance quantum, e is the electron charge and h is the Planck constant). Molecular junctions with such high and stable conductance are strongly desired for molecular electronics.

To date there are little information about the contact geometry and the details of the various orbital contributions to the transport in Ag-benzene-Ag junctions. In order to address these two aspects, here we investigate the binding configuration and the electronic transport properties of Ag-benzene-Ag junctions by employing the non-equilibrium Green's function formalism combined with density functional theory (in short the NEGF+DFT approach) [14-22]. Our calculations show that Ag-benzene-Ag molecular junctions can be formed when benzene is connected to Ag electrodes through either one or two Ag adatoms on each side. Although the contributions to the transmission around the Fermi level made by the different benzene molecular orbitals depend on the number of Ag adatoms and the binding

configurations, the total transmission coefficient at the Fermi level changes little. In particular we find transmission ranging between 0.16 and 0.20 in good agreement with the experimental value of 0.24±0.08 [10]. This confirms that Ag-benzene-Ag junctions can display a large and stable conductance.

2. Calculation method

The SIESTA code is used to study the atomic and electronic structures of the Ag-benzene-Ag molecular junctions, while the quantum transport code SMEAGOL is employed for their electronic transport properties. SIESTA is an efficient numerical implementation of DFT in which the wave functions of the valence electrons are expanded in terms of finite-range numerical basis sets [23], while improved Troullier-Martins pseudopotentials describe the atomic cores [24]. By means of extensive optimization a user-defined double-zeta plus polarization basis set is constructed for C and H and a single-zeta plus polarization one is used for Ag. The Perdew-Burke-Ernzerhof (PBE) generalized gradient approximation (GGA) for the exchange and correlation functional is used in all our calculations to account for the electron-electron interactions [25]. Geometry optimization is performed by conjugate gradient until the forces are smaller than 0.03 eV $Å^{-1}$.

SMEAGOL is a practical implementation of the NEGF+DFT approach [21,22]. Since SMEAGOL uses SIESTA as the DFT platform, we employ the same pseudopotentials, basis set and GGA functional for both geometry relaxation and transport. Periodic boundary conditions are applied in the transverse directions. The unit cell of the extended molecule comprises one benzene molecule and ten (111)-oriented Ag atomic layers with a (4×4) supercell. Furthermore, we use an equivalent cutoff of 200.0 Ry for the real space grid, while the charge density is integrated over 70 energy points along the semi-circle, 20 energy points along the line in the complex plane and 15 poles are used for the Fermi distribution (the electronic temperature is 25 meV). The transmission coefficient $T(E)$ of the molecular junctions is evaluated as

$$T(E) = \frac{1}{\Omega_{2DBZ}} \int_{2DBZ} T(\vec{k}; E) d\vec{k}, \quad (1)$$

where Ω_{2DBZ} is the area of the two-dimensional Brillouin zone (2DBZ) in the transverse directions. Here, we calculate the transmission coefficient by sampling 4×4 k-points in the transverse 2DBZ (orthogonal to the transport direction). The *k*-dependent transmission coefficient $T(\vec{k};E)$ is obtained as

$$T(\vec{k};E) = Tr[\Gamma_L G_M^R \Gamma_R G_M^{R+}], \qquad (2)$$

where G_M^R is the retarded Green's function matrix of the extended molecule and $\Gamma_{L(R)}$ is the broadening function matrix describing the interaction of the extended molecule with the left (right) electrode. More details on the calculation method can be found in reference [21,22].

3. Results and discussion

In order to determine the atomic details of the contact geometry, we first investigate the binding configurations of benzene horizontally adsorbed on the Ag(111) surface (the molecule plane is parallel to the surface). As shown in Fig.1, we have considered three different binding configurations which are respectively named Geometry I, IIA, and IIB. Here I and II indicate the number of Ag adatoms on the Ag(111) surface connected to benzene. The Ag adatoms are all located above the fcc three-fold hollow site of the Ag(111) surface which is represented by a slab model including three (111)-oriented Ag atomic layers with a (4×4) supercell. In Geometry I the Ag adatom is attached to benzene in a η^6-fashion. Then for the Geometry IIA each of the two Ag adatoms coordinates a C-C bond in the η^2-fashion, while in Geometry IIB these are respectively attached to one C atom in the η^1-fashion. The optimized C-Ag bond lengths and the corresponding binding energies for these three kinds of binding configurations are listed in Table 1. Here, the binding energy E_b is defined as E_b=E[benzene]+E[Ag_surface]–E[benzene+Ag_surface]. As we can see, the average C-Ag bond lengths range from 2.608 Å to 2.996 Å. Considering that the covalent radii of Ag and C are respectively 1.45±0.05 Å and 0.77 Å and that the corresponding van der Waals radii are 1.72 Å and 1.70 Å [26], we conclude that the adsorption of benzene on the Ag(111) surface through Ag adatoms is in between the covalent and

the van der Waals interaction. This is also corroborated by the calculated binding energies which are about 0.4~0.5 eV. Since the PBE GGA functional always underestimates dispersion interactions [27], the actual binding energies are likely to be slightly larger than those results reported here. Therefore, we can conclude that Ag-benzene-Ag junctions can be formed when one benzene molecule is attached to two Ag electrodes through Ag adatoms. For simplicity, we then construct three kinds of symmetric Ag-benzene-Ag junction models based on the above binding configurations, in which the second electrode is contacted to benzene in exactly the same way as the first one. Correspondingly, these junction models are termed as Junction I, IIA, and IIB. It should be noted that we have not considered the situation where benzene is adsorbed directly on the atomically flat Ag(111) surface since the binding energies are rather small [28].

We now move to investigate the electronic transport properties of the three Ag-benzene-Ag junctions. We start with Junction I (Fig.2a), in which the benzene molecule is connected to the Ag electrodes through one Ag adatom on each side. The corresponding equilibrium transmission spectrum is given in Fig. 2b. Since the distance between the two Ag adatoms is only 5.3 Å, direct tunneling may also contribute to the junction conductance. Therefore, the transmission spectrum of the Ag-vacuum-Ag junction without the benzene molecule is also given in Fig. 2b for comparison. As we can see, the rather small transmission coefficient of the Ag-vacuum-Ag junction in the energy range [-4.0 eV, 1.0 eV] demonstrates that benzene indeed plays an important role in the junction conductance. Although we find a high transmission plateau below -2.95 eV and two sharp transmission peaks centered respectively at -2.73 eV and 1.48 eV, the transmission around the Fermi level is not very large. In particular, the transmission coefficient at E_F is calculated to be 0.20. This is in good agreement with the experimental value of 0.24 [10].

A deeper insight into the conductance of Junction I can be obtained by projecting the transmission function onto the benzene molecular orbitals (Fig. 2c). This is obtained by using our previously developed projection method based on scattering states [29,30]. Since the Ag adatoms are connected to benzene in the η^6-fashion, the

local symmetry of benzene is preserved. Thus the highest occupied molecular orbital (HOMO) and the lowest unoccupied molecular orbital (LUMO) remain that of benzene in the gas phase, namely they are both doubly degenerate. Although the LUMO contributes a sharp transmission peak centered at 1.48 eV and the HOMO dominates both the sharp transmission peak at -2.73 eV and the large transmission plateau below -2.95 eV, they both provide a negligible contribution to the transmission around E_F (note that all energies are taken with respect to the Fermi level of the Ag electrodes). This instead originates from the HOMO-4 and HOMO-14 benzene states, a quite surprising result, considering that they both lie far below the Fermi level. Such a feature is also drastically different from the cases of benzene wired to metal electrodes through organic linker groups. For example, the low-bias conductance of the Au-diaminobenzene-Au junction is mainly contributed by the HOMO of the central molecule [5].

Such an interesting conduction mechanism of Junction I must be related with the specific geometrical structure. In Fig. 2d we present the local density of states (LDOS) of the Ag adatom. Below -2.3 eV, including both the sharp peak at -2.7 eV and the broad peak around -3.4 eV, the LDOS is dominated by the Ag 4d atomic shell, with the contribution from the Ag 5s atomic orbital increasing as the energy get larger and dominating at around E_F. When the energy further increases, the Ag 5p contribution appears and becomes comparable to that of the 5s atomic orbital in the energy range [0.75 eV, 2.0 eV]. Since the Ag 5s shell has spherical symmetry and the π-type benzene HOMO and LUMO have nodal planes perpendicular to the benzene plane, their interaction is symmetry-suppressed. As such both the HOMO and the LUMO cannot contribute to the transmission around the Fermi level. In contrast, the HOMO-4 and HOMO-14 states have no nodal planes perpendicular to the benzene plane. This is because the HOMO-4 state is the lowest occupied π-type benzene molecular orbital and the HOMO-14 state is a σ-type orbital constructed by the carbon sp^2-hybrids with the same phase sign (see Fig. 2c). As a result, the HOMO-4 and HOMO-14 states both interact strongly with the Ag 5s atomic orbital and thus dominate the transmission around E_F. In the same manner, the doubly degenerate

benzene HOMO interacts strongly with the Ag 4d atomic orbitals and dominates the sharp transmission peak at -2.73 eV and the high transmission plateau below -2.95 eV.

It is well known that molecular levels calculated by using local and semi-local exchange and correlation functionals (local density approximation, LDA, or GGA) are too high in energy due to the self-interaction error [27]. This may result in an incorrect alignment of molecular levels with the Fermi energy of the electrodes and thus an unphysical large transmission at around E_F. It is therefore interesting to explore whether or not the calculated large transmission coefficient around E_F for Junction I is genuine or simply an artifact of the self-interaction error contained in the PBE GGA functional. The atomic self-interaction correction (ASIC) scheme applied to the non-equilibrium quantum transport problem is used to carry out this analysis [31-35,11]. The ASIC corrections are only applied to benzene (C and H atoms), but not to Ag as the self-interaction error is small in metals. The empirical scaling factor α, which is a measure of the deviation of the ASIC potential from the exact SIC one, is set to be 0.83. This shifts the benzene HOMO downward in energy to -9.25 eV, which is the negative of the experimental ionization potential**.** The transmission curve, $T(E)$, of Junction I calculated with the ASIC method is shown in Fig. 3. As we can see, the overall shape of $T(E)$ in the energy range [-2.0 eV, 2.0 eV] follows closely that calculated with PBE, except that the transmission peak originating from the benzene LUMO is shifted from 1.48 eV to 0.35 eV. As a consequence $T(E_F)$ is still as high as 0.19, illustrating the robustness of the high transmission of Junction I. Since $T(E_F)$ receives contributions mainly from the HOMO-4 and HOMO-14 states of benzene, which couple strongly with the conducting states of the silver electrodes, it is expected that the self-interaction correction may be small around E_F. This is the reason for the stability of the large transmission coefficient at E_F to the choice of DFT functionals.

Next we investigate the transport properties of Junction IIA in which benzene is connected to the Ag electrodes through two Ag adatoms on each side in the η^2-fashion. The optimized atomic structure of Junction IIA and the corresponding equilibrium transmission spectrum together with the transmission projected onto the benzene molecular orbitals are shown in Fig. 4. This time $T(E_F)$ is calculated to be 0.18, i.e., it is only 10% smaller than that of Junction I. However, some changes do occur

concerning the contributions to the transmission made by the benzene molecular orbitals. Due to the presence of two Ag adatoms on each side, the local symmetry of benzene is much lowered and the degeneracy of its HOMO and LUMO is lifted. In particular, the doubly degenerate LUMO splits into two components: the orbital component having a nodal plane passing through two carbon atoms of the ring becomes the LUMO+1, while the other one becomes the sole LUMO. The LUMO state not only contributes to the transmission peak centered at 0.90 eV, but its tail also extends below the Fermi level. Thus, besides the HOMO-4, the LUMO also contributes to the transmission at the Fermi level. At variance with the case of Junction I, where the Ag adatoms interact equally with the six carbon atoms of benzene, the four Ag adatoms in Junction IIA have a much stronger interaction with the four carbon atoms bonded to them than with the other two. This is merely due to the different spatial proximity. Since the 2p atomic orbitals of these four carbon atoms constitute the LUMO with the same phase sign, the LUMO can now couple with the 4s atomic orbitals of the Ag adatoms and thus contributes to the transmission around E_F.

Finally we would like to investigate the transport properties of Junction IIB, where benzene is connected to the Ag electrodes through two Ag adatoms on each side but in the η^1-fashion. The equilibrium transmission spectrum of Junction IIB is presented in Fig. 5, together with the transmission projected onto the benzene molecular orbitals. The overall shape of the transmission curves of these two junction models is almost identical, except that the transmission peaks contributed by the benzene LUMO and LUMO+1 are well separated in Junction IIB whereas they are merged into a single one for Junction IIA. In Junction IIB $T(E_F)$ is still dominated by the LUMO and HOMO-4 of benzene. Although the reason for the LUMO of benzene contributing to the transmission around the Fermi level is similar for Junctions IIA and IIB, in Junction IIB only two carbon atoms in the benzene ring interact strongly with the Ag adatoms. Compared with Junctions I and IIA, the transmission coefficient at the Fermi level of Junction IIB is decreased a little further and reaches 0.16. Certainly, this value is consistent with the measured one.

4. Conclusion

In this work we have investigated the contact geometry and the electronic transport properties of Ag-benzene-Ag junctions. Because moderate benzene-silver interaction can be achieved only when the benzene molecule is adsorbed on the Ag(111) surface through Ag adatoms, three kinds of symmetric Ag-benzene-Ag junction models are constructed. For the Ag-benzene-Ag junction where one Ag adatom contacts benzene in the η^6-fashion, $T(E_F)$ is calculated to be 0.20, in good agreement with the experimental value of 0.24. Since the 4s atomic shell of the Ag adatom dominates its LDOS around the Fermi level, the doubly degenerate benzene HOMO and LUMO cannot make contributions to the transmission around E_F due to symmetry mismatch. In contrast, the HOMO-4 and HOMO-14 states, which have no nodal planes perpendicular to the benzene plane, interact strongly with the 4s atomic orbital and thus dominate $T(E_F)$. For the other two Ag-benzene-Ag junctions having two Ag adatoms on each side contacting benzene in either η^2- or η^1-fashion, the local benzene symmetry is much lowered and the degeneracy of the HOMO and LUMO is lifted. Besides the HOMO-4, one orbital component of the LUMO, which has no nodal plane passing through the carbon atoms in the benzene ring, couples with the 4s atomic shell of the Ag adatoms and thus contributes to the transmission around E_F. The transmission coefficients of these two junction models at the Fermi level are calculated to be 0.18 and 0.16, respectively, illustrating that the low-bias conductance of the Ag-benzene-Ag junction is not affected significantly by the contact geometry even though the details of the contributions to the transmission around the Fermi level made by the various molecular orbitals depend somewhat on the contact geometry.

Acknowledgement

This project was supported by the National Natural Science Foundation of China (No. 61071012) and the MOST of China (No. 2011CB933001). The SMEAGOL project (SS) is sponsored by Science Foundation of Ireland (07/IN.1/I945) and by CRANN.

Reference

[1] N.J. Tao, Nat. Nanotechnol., 1, 173(2006)

[2] R. L. McCreery, A.J. Bergren, Adv. Mater., 21, 4303(2009)

[3] M.A. Reed, C. Zhou, C.J. Muller, T.P. Burgin, J.M. Tour, Science, 278, 252(1997)

[4] L. Venkataraman, J.E. Klare, I.W. Tam, C. Nuckolls, M.S. Hybertsen, M.L. Steigerwald, Nano Lett., 6, 458(2006)

[5] J. Ning, R. Li, X. Shen, Z. Qian, S. Hou, A.R. Rocha, S. Sanvito, Nanotechnology, 18, 345203(2007)

[6] Y.S. Park, A.C. Whalley, M. Kamenetska, M.L. Steigerwald, M.S. Hybertsen, C. Nuckolls, L. Venkataraman, J. Am. Chem. Soc.,129, 15768(2007)

[7] M. Kiguchi, S. Miura, K. Hara, M. Sawamura, K. Murakoshi, Appl. Phys. Lett., 91,053110 (2007)

[8] R. Zhang, G. Ma, M. Bai, L. Sun, I. Rungger, Z. Shen, S. Sanvito, S. Hou, Nanotechnology, 21, 155203(2010)

[9] M. Kiguchi, O. Tal, S. Wohlthat, F. Pauly, M. Krieger, D. Djukic, J. C. Cuevas, J. M. van Ruitenbeek, Phys. Rev. Lett., 101, 046801(2008)

[10] S. Kaneko, T. Nakazumi, M. Kiguchi, J. Phys. Chem. Lett., 1, 3520(2010)

[11] G. Ma, X. Shen, L. Sun, R. Zhang, P. Wei, S. Sanvito, S. Hou, Nanotechnology, 21, 495202(2010)

[12] Z.-L. Cheng, R. Skouta, H. Vazquez, J.R. Widawsky, S. Schneebeli, W. Chen, M.S. Hybertsen, R. Breslow, L. Venkataraman, Nat. Nanotechnol., 6, 353(2011)

[13] S.T. Schneebeli, M. Kamenetska, Z. Cheng, R. Skouta, R.A. Friesner, L. Venkataraman, R. Breslow, J. Am. Chem. Soc.,133, 2136(2011)

[14] Y. Meir, N.S. Wingreen, Phys. Rev. Lett., 68, 2512(1992)

[15] P. Hohenberg, W. Kohn, Phys. Rev., 136, B864(1964)

[16] W. Kohn, L.J. Sham, Phys. Rev., 140, A1133(1965)

[17] Y. Xue, S. Datta, M.A. Ratner, Chem. Phys., 281, 151(2002).

[18] M. Brandbyge, J.-L. Mozos, P. Ordejón, J. Taylor, K. Stokbro, Phys. Rev. B, 65, 165401(2002).

[19] J. Zhang, S. Hou, R. Li, Z. Qian, R. Han, Z. Shen, X. Zhao, Z. Xue, Nanotechnology, 16, 3057(2005).

[20] R. Li, J. Zhang, S. Hou, Z. Qian, Z. Shen, X. Zhao, Z. Xue, Chem. Phys., 336, 127(2007)

[21] A.R. Rocha, V.M. Garcia-Suarez, S.W. Bailey, C.J. Lambert, J. Ferrer, S. Sanvito, Nature Mater., 4, 335(2005)

[22] A.R. Rocha, V.M. García-Suárez, S. Bailey, C. Lambert, J. Ferrer, S. Sanvito, Phys. Rev. B, 73, 085414(2006).

[23] J.M. Soler, E. Artacho, J.D. Gale, A. García, J. Junquera, P. Ordejón, D. Sánchez-Portal, J. Phys.: Condens. Matter, 14, 2745(2002)

[24] N. Troullier, J. Martins, Phys. Rev. B, 43, 1993(1991)

[25] J. Perdew, K. Burke, M. Ernzerhof, Phys. Rev. Lett., 77, 3865(1996)

[26] A. Bondi, J. Phys. Chem., 68, 441(1964)

[27] W. Koch, M.C. Holthausen, A Chemist's Guide to Density Functional Theory, second edition, Wiley-VCH, Weinheim, 2001

[28] A. Bilić, J.R. Reimers, N.S. Hush, R.C. Hoft, M.J. Ford, J. Chem. Theory Comput., 2, 1093(2006)

[29] R. Li, S. Hou, J. Zhang, Z. Qian, Z. Shen, X.J. Zhao, J. Chem. Phys., 125, 194113(2006)

[30] S. Hou, Y. Chen, X. Shen, R. Li, J. Ning, Z. Qian, S. Sanvito, Chem. Phys., 354, 106(2008)

[31] C.D. Pemmaraju, T. Archer, D. Sánchez-Portal, S. Sanvito, Phys. Rev. B 75, 045101(2007)

[32] C. Toher, S. Sanvito, Phys. Rev. Lett., 99, 056801(2007)

[33] C. Toher, S. Sanvito, Phys. Rev. B, 77, 155402(2008)

[34] R.B. Pontes, A.R. Rocha, S. Sanvito, A. Fazzio, A.J.R. da Silva, ACS Nano, 5, 795(2011)

[35] P. Wei, L. Sun, E. Benassi, Z. Shen, S. Sanvito, S. Hou, J. Chem. Phys., 134, 244704(2011)

Table I The average C-Ag bond lengths and binding energies of the benzene molecule adsorbed on the Ag(111) surface through Ag adatoms

Binding configuration	Binding energy (eV)	C-Ag bond length (Å)
Geometry I	0.41	2.996
Geometry IIA	0.52	2.720
Geometry IIB	0.52	2.608

Figure captions

Figure 1 The optimized atomic structures of a benzene molecule adsorbed on the Ag(111) surface through one or two Ag adatoms. From left to right: Geometry I, IIA and IIB

Figure 2 (a) The optimized atomic structure of Junction I; (b) the equilibrium transmission spectrum (solid blue line) of Junction I, and the equilibrium transmission spectrum (dash red line) of the Ag-vacuum-Ag junction without benzene is also given for comparison; (c) the transmission projected onto molecular orbitals of benzene and the HOMO-4 and HOMO-14 states of benzene (the positions of the Ag adatoms are also shown); (d) the LDOS of the Ag adatom in Junction I

Figure 3 The equilibrium transmission spectrum of Junction I calculated with the ASIC scheme, the transmission spectrum calculated with the PBE GGA functional is also given for comparison

Figure 4 (a) The optimized atomic structure of Junction IIA; (b) the equilibrium transmission spectrum of Junction IIA together with the transmission projected onto molecular orbitals of benzene, and the HOMO-4 and LUMO states of benzene (the positions of the Ag adatoms are also shown)

Figure 5 The equilibrium transmission spectrum of Junction IIB together with the transmission projected onto molecular orbitals of benzene, and the HOMO-4 and LUMO states of benzene (the positions of the Ag adatoms are also shown)

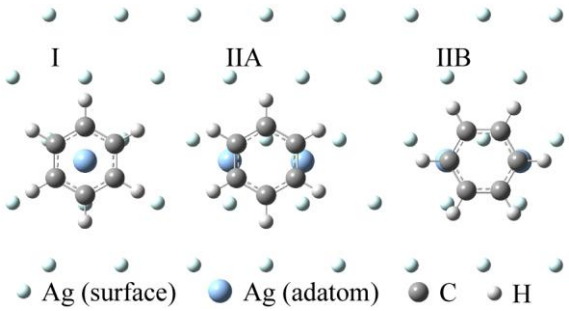

Figure 1

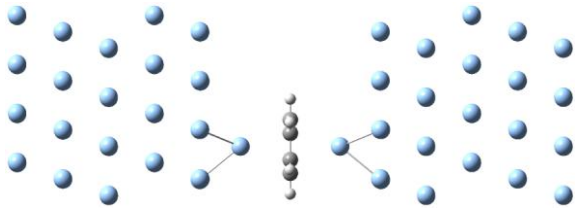

(a)

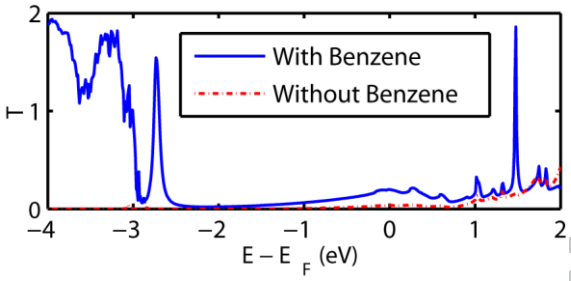

(b)

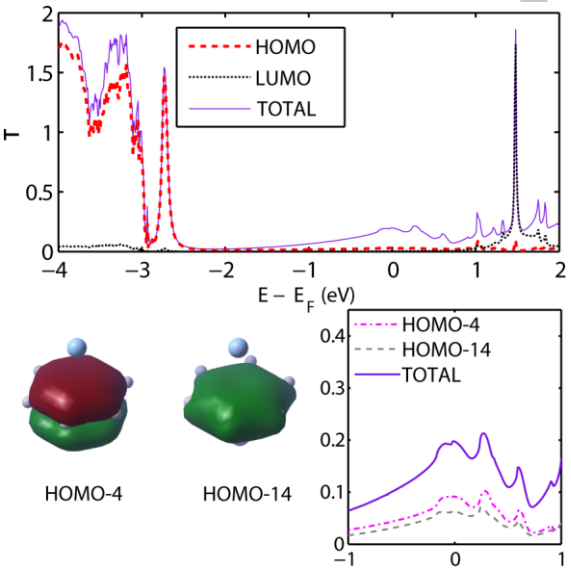

(c)

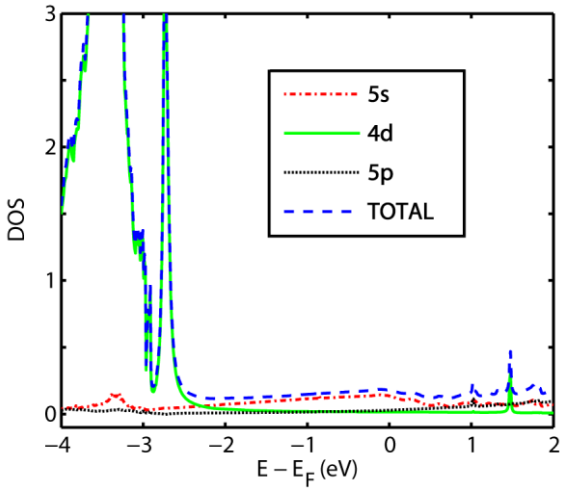

(d)

Figure 2

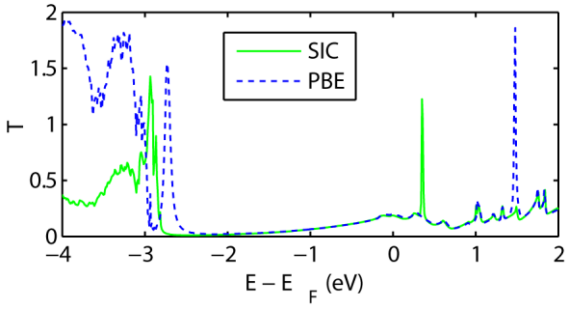

Figure 3

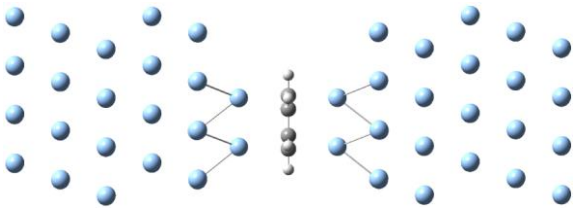

(a)

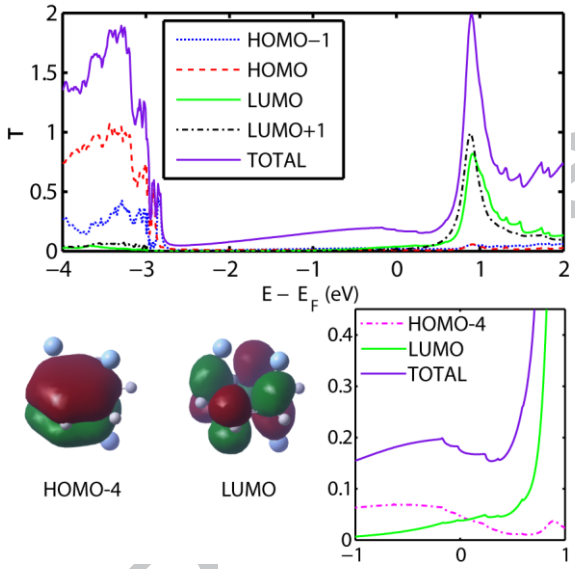

(b)

Figure 4

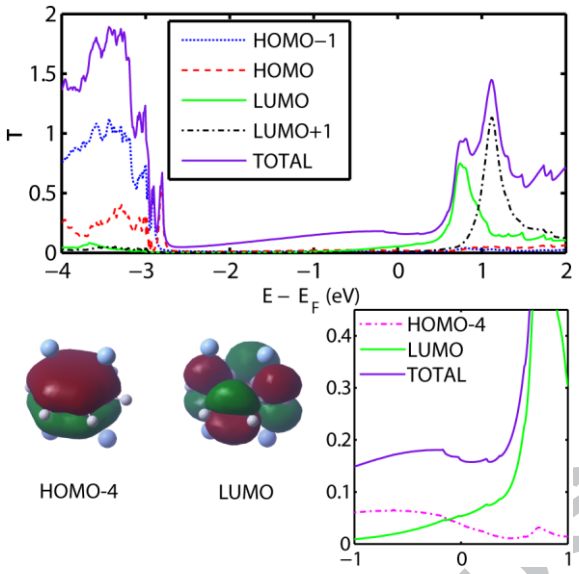

Figure 5

*Graphical Abstract (pictogram)

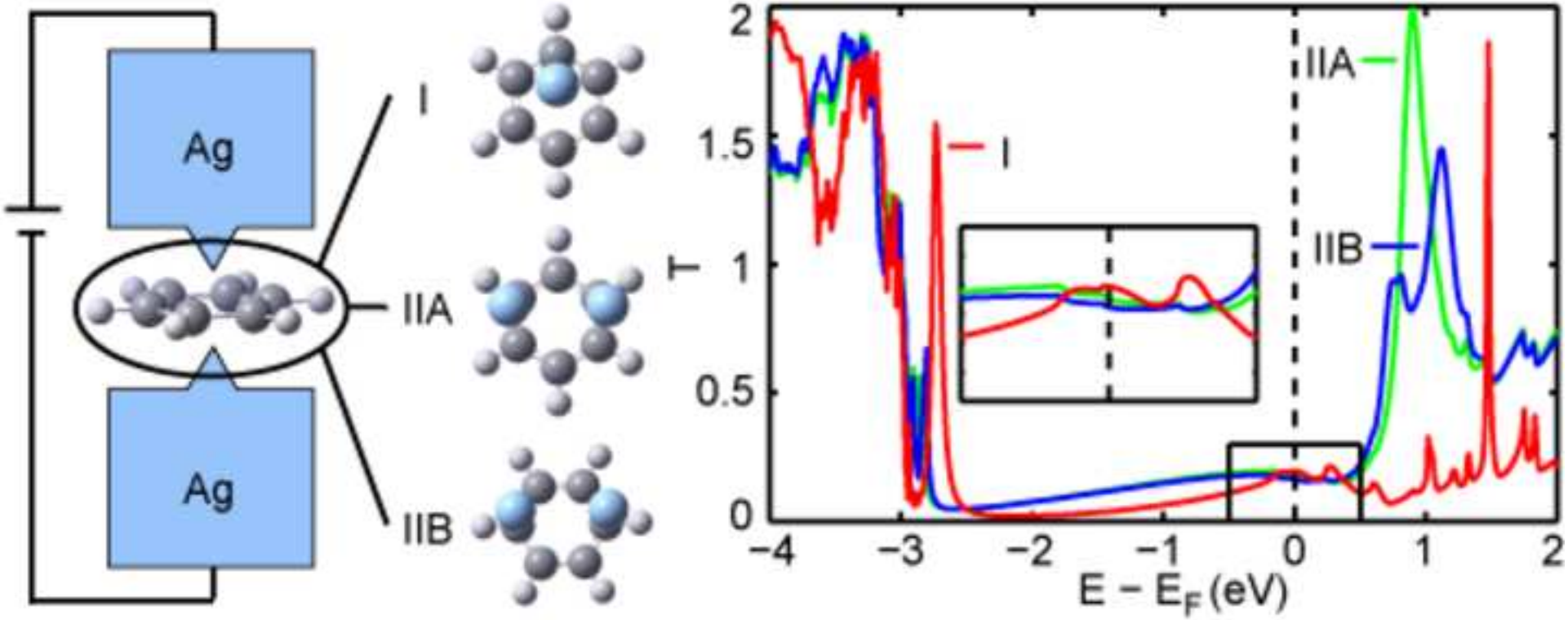

***Graphical Abstract (synopsis)**

Fixed conductance value can be achieved for Ag-benzene-Ag junctions with different contact geometries.

*Highlights

> We simulate Ag-benzene-Ag junctions with different contact geometries. > Moderate benzene-Ag interactions can be realized for adsorptions through Ag adatoms. > Molecular orbitals dominating the low-bias conductance match the contact symmetry. > Three contact geometries deliver similar conductance consistent with experiments.